Real-time Flood Mapping on Client-side Web Systems using HAND model

Anson Hu [1], Ibrahim Demir [2],*

[1] Computer Science, Massachusetts Institute of Technology
[2] Civil and Environmental Engineering, University of Iowa
* Corresponding Author: ibrahim-demir@uiowa.edu

Abstract: The height above nearest drainage (HAND) model is frequently used to calculate properties of the soil as well as predict flood inundation extents. HAND is extremely useful due to its lack of reliance on prior data, as only the digital elevation model (DEM) is needed. It is close to optimal, running in linear or linearithmic time in the number of cells depending on the values of the heights. It can predict watersheds and flood extent to a high degree of accuracy. We applied a client-side HAND model on the web to determine extent of flood inundation in several flood prone areas in Iowa, including city of Cedar Rapids and Ames. We demonstrated that the HAND model was able to achieve inundation maps comparable to advanced hydrodynamic models (i.e. FEMA-approved Flood Insurance Rate Maps) in Iowa, and would be helpful in the absence of detailed hydrological data. The HAND model is applicable in situations where a combination of accuracy and short runtime are needed, for example, in interactive flood mapping and supporting mitigation decisions, where users can add features to the landscape and see the predicted inundation.

Keywords: flood maps; flood risk management; HAND model; WebAssembly; flood risk mapping; web systems; floods; urban flooding; flood analysis

1. Introduction

Flooding is a global problem, and floods around the world are becoming more significant and severe [1]. 40% of natural disasters worldwide are floods [2]. It is important to model and predict inundation extent of floods, which is critical information for flood mitigation [3-4], preparedness [5], and planning and response efforts [6]. Real-time and accurate predictions of flood inundation extent can facilitate understanding the potential flood risk and damage [7-8], and support flood mitigation and planning. Flood inundation maps can be used in flood risk communication using intelligent systems [9-10] and novel communication systems [11].

Floods are caused by a multitude of factors, which makes prediction difficult [12]. Moisture flows and consequently rainfall [13], runoff and stream behavior [14] and other issues affect flooding significantly. For these reasons, flood prediction has a highly complex and non-linear nature [15]. There are various models to predict flood extent. While empirical models include observations [16] and remote sensing [17], and benchmark datasets [18] of past events, hydrodynamic models simulate physical movement of the water [19]. Data driven methods are used extensively in hydrology and water resources modeling [20-21]. One of the simplest and earliest data driven methods based on elevation is flood-fill, which produces results in optimal time but provides less accurate predictions. Another simple method involves overlaying an observed flood level with the topography [22]. On the other hand, there are a variety of complex hydrological models that take into account numerous distinct factors, such as the three-dimensional model [23]. Generally, models that have a good balance between speed and accuracy are used in operational needs [24]

There are several challenges with the existing hydrodynamic models to be helpful in real-time and operational decision-making situations [25]. One of the main issues is that these models often require a lot of detailed hydrological data [26]. For example, advanced hydrodynamic models for flood map prediction often take into account a plethora of factors, including riverbed dynamics, hydraulic features and structures [27]. The second main challenge to utilize these models in decision making is their computational complexity. Some of the methods that provide a balance between speed and accuracy [28] also utilize data that is costly to gather, such as topographical indices [29].

The height above the nearest drainage algorithm has a wide variety of applications. HAND was originally designed to categorize soil environments and find water tables. Renno et al [30] first outlined the algorithm and applied it to categorize swampy forests vs. terra-firme forests in the Amazonian jungle. Nobre et al [31] applied HAND to categorize water tables in a large area of the central Amazon rainforest. The most recent application area for HAND methods is in flood inundation. Nobre et al [32] applied the HAND model to predict flooding in Southern Brazil. The largest application of this is being able to predict flooding in areas that have little to no prior data, due to the HAND model's total reliance on the DEM. Previous studies on HAND model to predict flood maps [32] achieved model accuracy around 86-98% when compared to reference flood extent maps.

Recent advancements in web technologies have allowed for desktop level computation and analysis of large-scale datasets. Web systems have been effectively used in environmental data analysis [33-34], distributed computing [35], and geo-spatial data processing [36]. WebAssembly is a low-level assembly-like language for the web with near-native performance

and allows languages such as C/C++, C# and Rust to run on the web. WebAssembly was recently released in March 2017 and is designed to run code both safely and efficiently in browsers on the client-side [37]. These technologies have allowed for previously unobtainable speeds and computations to be performed on local users' computers.

Here, we utilize the HAND method in order to provide flood inundation extent predictions in real-time on client-side web systems. We discuss the applicability of the algorithm in comparison with other prediction algorithms for flood-prone regions of Iowa and the applications for such real-time prediction. Our objective is to outline the HAND algorithm and demonstrate that it has potential to predict both accurately and quickly on the web, and support flood related decision-making activities [38-39]. There are a variety of benefits that HAND can provide in flood inundation prediction. First, due to its low complexity, HAND runs in very fast time both theoretically and practically. This means that stakeholders involved or interested in flood planning (for example a government official or concerned citizen) can easily make changes to a DEM to simulate adding man-made barriers and then run the algorithm to determine how these changes affect flood inundation extents. This can lead to more effective flood protection planning, since previously users were meant to look at a standalone flood model generated once by an advanced but computationally expensive algorithm and then make educated guesses on the design and utilization of man-made flood prevention measures.

In the following sections, we will outline the algorithm, details of implementations on the web systems, and several evaluation case-studies for comparison to real-world flooding scenarios.

2. Materials and Methods

Our goal with this study is to demonstrate the implementation of the HAND model on client-side web systems and evaluate the accuracy and performance for real-time decision-making scenarios. The system will provide an implementation of the HAND algorithm that runs in the local browser of the user for fast flood extent prediction that can work offline and in operational settings with minimal processing on the web server. The system will allow users to modify aspects of the terrain for mitigation purposes and be able to see predicted flood inundation extents in order to facilitate the use of measures to control potential flood damage.

2.1. Web Implementation of HAND

Figure 1 presents the architecture of the real-time web-based HAND flood map generation system. It includes several steps to compute and generate flood maps using the HAND algorithm. The system is designed so that the algorithmic portion of HAND is entirely in C++ and run on WebAssembly to enable client-side implementation. The code for the computationally heavy portion of the HAND algorithm was written in C++. Emscripten was used to compile the C++ code to WebAssembly, which allows JavaScript (JS) to pass input data and receive model output. The only input is the DEM data and the drainage threshold value provided by the user. The WebAssembly-compiled implementation of HAND calculates the heights above nearest drainages and passes that information to JavaScript for visualizing the flood extent on Google Maps.

The C++ algorithmic implementation is precompiled into WebAssembly. The resulting code is meant to supply an efficient way to run the HAND algorithm. Most features of prediction which can be applied either pre- or post-computation are left out of the WebAssembly component. WebAssembly is running on an in-browser virtual machine. JavaScript glue code generated by Emscripten provides a means to interface with the WebAssembly VM. The HTML/JS frontend loads images from a source, either static or online, and applies user selected parameters before and after computation. This piece of the architecture calls the API provided by the glue code to interface with the WebAssembly VM and provide prediction results. The JS manages the frontend of the application for taking user inputs, integrating external terrain data, and visualizing map output.

The web implementation is meant to make the system as flexible as possible for all sorts of applications that can utilize the HAND algorithm implementation, and apply their own features (changing terrain, allowing for multiple parameter changes in local areas, etc.). For example, one application might scrape DEM data from various online sources and allow users to generate flood maps in any region in the world. A different application might generate DEMs with another algorithm and allow users to explore the generated flood maps.
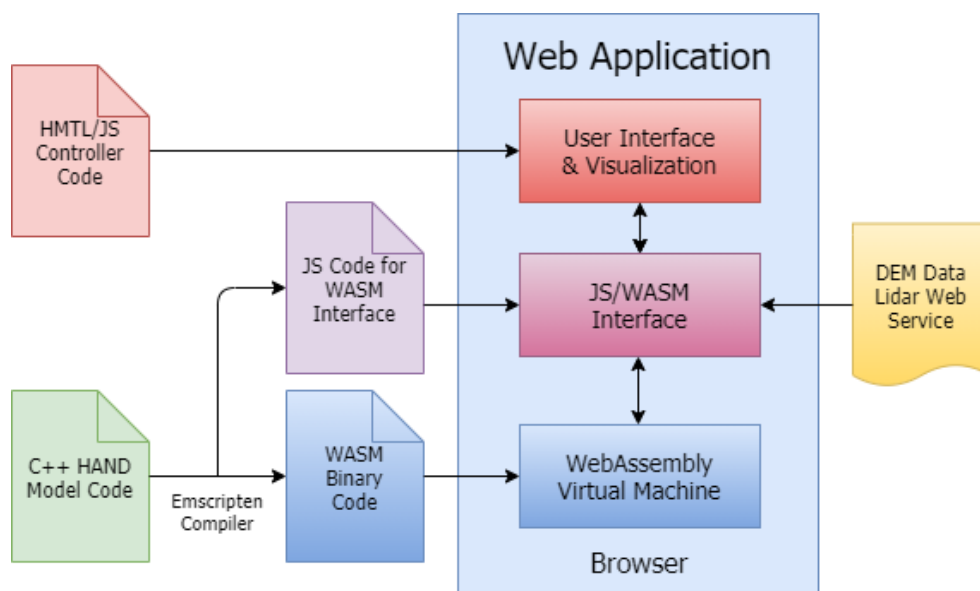
Figure 1. Architecture and components of the real-time web-based HAND system

Many of the features relevant for flood prediction are nearly independent of the computation of the HAND. For example, two of the three relevant parameters, HAND threshold and absolute height threshold, can be applied after actual HAND model is computed. In addition, other features such as applying HAND thresholds only to specific areas, dynamically loading DEMs, and adding terrain features (dikes, reservoirs, etc.) are better suited to the client-side processing using JavaScript. Because these features are highly application-specific but low in terms of computational expense, we leave them out of the C++ and WebAssembly implementation. For example, one application might require dynamic loading of DEMs from state resources, while another generates DEMs with an algorithm and passes them in. This allows the C++ implementation to be highly portable and versatile; a wide variety of applications requiring the use of the HAND algorithm can utilize it.

2.2. HAND Algorithm

In our study, we applied HAND methodology (as described in [31-32]) in order to predict the extent of flood inundation. By calculating the vertical distance from a cell and its parent cell and applying several heuristic steps, we can calculate the extent of flood inundation with a comparable accuracy. A brief description of the steps for HAND algorithm is given here:

<u>Determining Flow Direction:</u> We define the direction of the flow of a cell a in the DEM as the adjacent cell to which the water on a will flow. Water can only flow in one direction, which means that it can only flow to one cell. We define the set of adjacent cells to the cell at coordinates (x0, y0) in Equation 1 as

$$\{ (x, y) \mid \max (|x - x0|, |y - y0|) = 1 \} \tag{1}$$

We define the child of a cell a to be the cell b such that the direction of the flow of cell a is towards cell b. We define a flow chain of a cell a as an ordered list of cells such that the first cell in the list is a, and each subsequent cell is a child of the previous cell.

<u>Depression Removal:</u> First, the graph must be normalized to remove depressions that are undrainable. An undrainable depression is a set of cells in which any pair of cells in the set can be reached by traversing a path of cells in which consecutive cells on the path are adjacent to each other and each cell in the path is part of the set and none of the cells have a continuous flow to the border of the DEM (none of the cells have a border cell in their flow chain). We used priority-flood depression filling [40] in this case. This ensures that all water can drain to the outside of the map, and that there will be no cycles or other anomalies that can disrupt subsequent algorithms. This step runs in O(N) for integer elevations or O(N log N) for floating-point elevations, where N is the number of cells.

<u>Computing Flow Directions:</u> Then, the direction of water flow for each cell needs to be resolved. We used the D8 algorithm to compute the flow directions. The D8 algorithm takes the adjacent cell that provides the highest gradient to be the cell of the direction of the flow. A flat-resolving algorithm [41] was used to determine direction of flow in flat areas (where all adjacent cells to a cell have the same height) and guide water away from high areas and towards lower areas. This step runs in O(N) time.

<u>HAND Model Generation:</u> Next, drainages need to be established on the graph. This is done by setting an accumulated area threshold. If a cell has more units of area of water that drain through it than the area threshold, then it becomes a drainage cell. In other words, if the number of flow chains that the cell is part of is greater than the accumulated area threshold, then it is a drainage cell. The nearest drainage for a cell is then the first cell in its flow chain that is a drainage cell. This step runs in O(N) time. Finally, the heights above the nearest drainage are calculated by subtracting the height of the cell in the original DEM with the nearest drainage cell's height in the original DEM.

*2.3. Implementation Challenges*

There were several issues encountered during the course of implementing the HAND model on the web. HAND model does not account for some of the parameters like height of water and absolute height.

Height of Water: The HAND algorithm as it currently exists views each drainage stream as only one pixel in width, and it does not take into account the height of water. This means that the algorithm will think that a wide river is actually a canyon. The algorithm thinks that the banks of the river have extremely high HAND values because the stream's elevation is at the bottom of the river. In reality the banks of the river have HAND value near zero, because water goes up to the top of the river bank, but the algorithm does not reflect this. To overcome this issue, we have added two parameters into implementation.

a) HAND flood threshold (hereafter referred to as "HAND threshold"). This is the main component of the flood inundation calculation. If the HAND of a cell is below this threshold, then it will be counted as flooded, as long as it satisfies the third parameter. In other words, a cell a is counted as flooded by threshold t if HAND[a] < t.

b) Accumulated area of drainage threshold (hereafter referred to "drainage threshold"). This is used to define which flows of water are actually drainages. If the amount of water area that flows over a cell is over this threshold, then it is counted as a drainage.

There are several effects of these parameters on the model outcome. As the HAND threshold goes up, the extent of areas marked as flooded will increase. If the HAND threshold is defined too high, the entire area will be flooded. Drainage threshold controls how many drainage points are available in the selected region. If the drainage threshold is defined too high, the algorithm becomes a slow flood-fill. If it is too low, the flooding predictions are exceedingly coarse, with big blotches splattered around with general inaccuracy. By having a high HAND threshold and enough drainage streams, we allow the areas adjacent to the rivers to be easily flooded, despite being viewed as canyons by the algorithm.

Absolute Height: If there is a large plateau that drains into a stream going downhill, the algorithm will view the plateau as flooded, even when it might be far above local rivers and other water bodies and have a low chance of flooding. To overcome this issue, we have added a third parameter for the maximum height threshold of flooding (hereafter referred to "absolute height threshold"). If a cell's absolute height is above this threshold, then it will not be considered as flooded. Absolute height threshold controls extent of flooding. If it is defined too high, areas that would be dry are predicted as flooded. If it is too low, the algorithm will miss much of the flooding in higher areas. A medium absolute height threshold allows rivers that have a slope to still have effective flooding predictions within them and on their borders but prevents adjacent flat-but-elevated landforms being counted as flooded. A combination of a medium absolute height threshold and high HAND threshold effectively serves to counter the two issues listed.
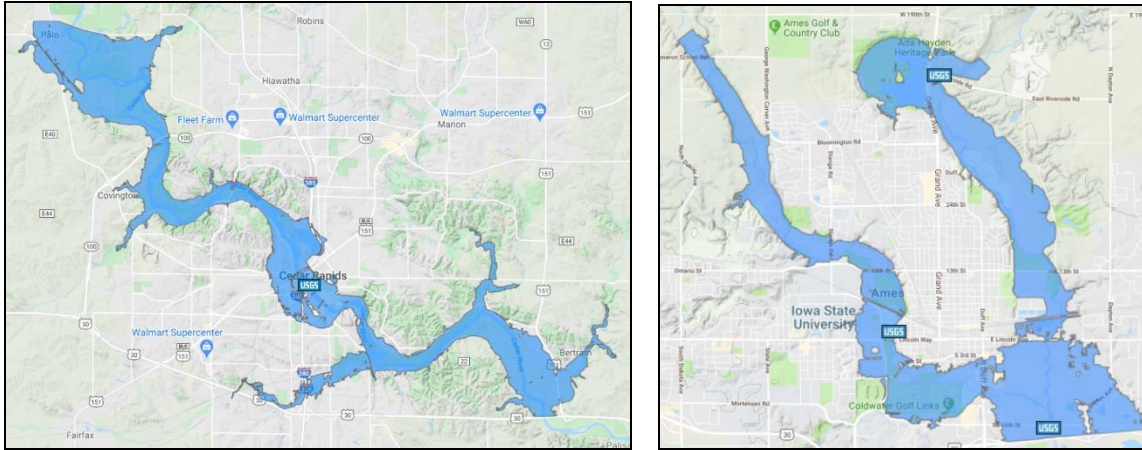
Figure 2. FEMA-approved flood maps for Cedar Rapids (left) and Ames (right), Iowa by IFC

3. Results and Discussion

We compared the results of the HAND output with two other flood inundation predictors: a basic flood-fill implementation and FEMA-approved Flood Insurance Rate Maps developed [42] at the Iowa Flood Center (IFC). We used two datasets for the analysis. The first was the Cedar Rapids (Figure 2) metro area in Iowa, where we utilized a DEM at a resolution of 1 meter for 5 sq km area (2863 x 1746 grid). The second was for the Ames, Iowa (Figure 2), where we used a DEM of at a resolution of 2 meters for 53.8 sq km area (4220 x 3189 grid). All DEMs were normalized to 255 units corresponding to 1 to 3 ft vertical elevation in real-world based on vertical resolution.
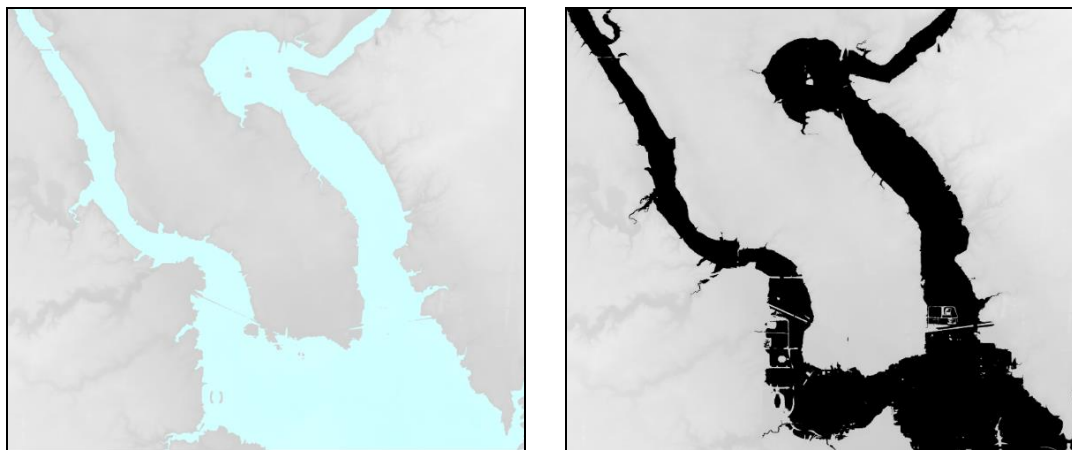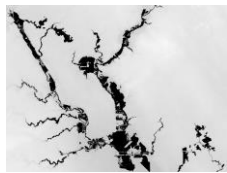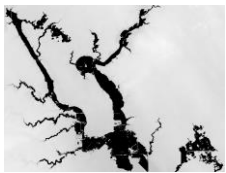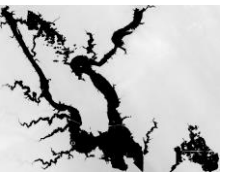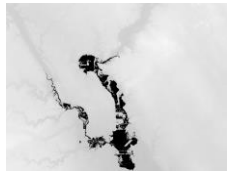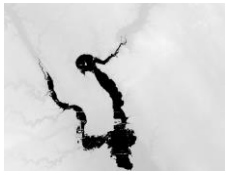

Figure 3. Maps generated for Ames using basic flood-fill (left) and HAND model (right)

For the Cedar Rapids area, the HAND algorithm ran in roughly 3 seconds using a mid-range personal laptop and produced an output differing from the reference map predictions by 10%. The flood-fill implementation ran in less than one second and produced an output differing by roughly 15%. For the Ames area, the HAND algorithm (Figure 3) ran in roughly 9 seconds and produced an output differing from the reference map predictions by 6%. The flood-fill implementation (Figure 3) ran in roughly one second and produced an output differing by roughly 30%. The HAND model's accuracy was notably improved, both in absolute error and in

error relative to the flood-fill implementation; this was most likely due to the larger scale of the Ames DEM. Comparisons were drawn between appropriate thresholds in the FEMA reference maps and the results of the HAND implementation. Several predictions of arbitrary values of parameters were generated with the algorithm and are presented here to show the effects of adjusting the parameters of the prediction algorithm on the output.

Table 1. Sensitivity of model parameters on flood extent (absolute threshold 220 ft)

Drainage Threshold	HAND Threshold			
	2	3	4	6
100k cells				
500k cells				
1m cells				
2m cells				
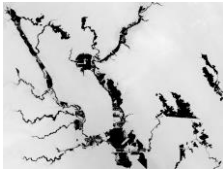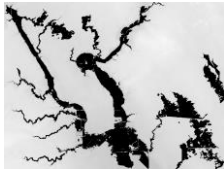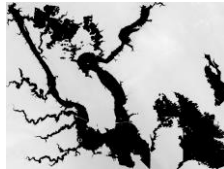
3.1. Adjustment of Parameters

To adjust for flood predictions in areas without prior predictions or flood maps, we must take into account the scale of the area we are modifying, as well as a sense of an absolute maximum for good area control. The Ames area DEM measures 65 square km, and the most effective drainage threshold measured was 1 million cells corresponding to a 4 square km area. This is most likely the absolute maximum, as it is strikingly similar to suggested effective threshold value of 4.05 square km in the literature [32]. The HAND threshold is highly correlated with the level of the flooding on the terrain. The best way to analyze this is to figure out the relative heights of the cells and compare them to real-world heights, and then scale appropriately. For example, if the cells had relative heights corresponding to one unit as 2 ft, and if information exists that areas less than 4 ft above the nearest drainage will be flooded, then the HAND threshold can be set as two units corresponding to 4 ft.

The absolute threshold must be determined by the maximum height that the user predicts the flood will extend, similar to the HAND threshold, but in an absolute manner. To generalize parameters to areas for which there is no prior prediction available, it is recommended that areas with similar topography and known predictions for flood inundation extents be examined; then, user can find good parameters for the HAND algorithm that match those known predictions, and apply those same parameters to the unknown area.

Table 2. Sensitivity of model parameters on flood extent (absolute threshold 225 ft)

Drainage Threshold	HAND Threshold			
	2	3	4	6
100k cells				
500k cells				
1m cells				
2m cells				

3.2. Evaluation of Parameter Sensitivity

We have evaluated the sensitivity of the HAND parameters on generating the flood extent. Table 1 and 2 presents the resulting flood extents for changing model parameters mentioned in the HAND algorithm section above. We have tested several drainage threshold values (100K, 500K, 1M, 2M cells), HAND threshold (2, 3, 4, 6 units), and absolute elevation threshold (220, 225 ft) values. As seen from the resulting flood extents, higher HAND threshold values cause larger areas around drainage points to be flooded. Higher drainage threshold on the other hand causes number of drainage points to be fewer which causes less branching in the predictions. Higher absolute threshold causes fewer high-elevation areas to be flooded.

3.3. Real-time HAND Generation Performance

We have evaluated the computation performance of client-side flood map generation using HAND model and WebAssembly. We have selected different DEM resolutions (1, 5, 10, 25, 50, 100m) and grid size (1, 4, 9, 16, 25 million cells). Based on the selected elevation data resolution and grid size, generated maps represent city, county and state scale in coverage (Table 3). The performance of the map generation takes roughly 0.25 to 6.25 seconds on a moderate personal computer. Higher DEM resolutions could be used for any scale based on data availability and computing resources. The client-side implementation on WebAssembly could further speed up by using Web Workers and distributing the computation to multiple CPUs on the same machine.

Table 3. Computational time for generating flood extent in different scales and resolutions

Scale	DEM Resolution	Region	Grid Cells	Computing Time
City	1 – 5m	1 – 225 sq km	1 – 9 million	0.25 – 2.25 sec
County	5 – 10m	225 – 1,600 sq km	9 – 16 million	2.25 – 4.00 sec
State	25 – 100m	10,000 – 250,000 sq km	16 – 25 million	4.00 – 6.25 sec

4. Conclusions

Real-time flood map generation is critical for operational activities in flood preparedness, mitigation and response. Traditional flood mapping models requires extensive data and computation resources. In this study, we have presented real-time flood map generation in client-side web systems using HAND model with comparable results to FEMA-based reference maps. The height above the nearest drainage model computes the vertical distance from each cell to its nearest drainage. Testing of the HAND model in two key regions of Iowa demonstrated that the HAND model can be used to generate flood inundation predictions that are both accurate and fast. Predictions generated matched precomputed FEMA-approved Flood Insurance Rate Maps with acceptable accuracy within several seconds. Previous papers and applications of HAND focused on their minimal usage of external datasets, which allows for prediction of soil conditions and flood inundation extent in areas with little to no data aside from elevation datasets. The main application of our development is the ability of floodplain managers and end-users to add features to the terrain, such as levees and reservoirs, and examine how they will affect the extent of flooding. Because the users will be able to modify the terrain and see the result in real time, they will be able to get a better idea of how flood mitigation measures will affect flood inundation extents and be able to prepare for flooding in time with more accurate and relevant information. Future work can include an interactive user interface allowing selection of parameters, with potential automation and algorithms to select parameters to reflect real-world scenarios.

References

1. Coumou D, Rahmstorf S. 2012. A decade of weather extremes. Nature Climate Change 2: 491–496. DOI: 10.1038/nclimate1452.
2. Noji, E.K. 1991. "Natural Disasters." Critical Care Clinics 7 (2): 271–92.
3. Bhola, P.K., Leandro, J. and Disse, M., 2018. Framework for offline flood inundation forecasts for two-dimensional hydrodynamic models. Geosciences, 8(9), p.346.
4. Tadesse, Y.B. and Fröhle, P., 2020. Modelling of Flood Inundation due to Levee Breaches: Sensitivity of Flood Inundation against Breach Process Parameters. Water, 12(12), p.3566.
5. Arrighi, C., Pregnolato, M., Dawson, R.J. and Castelli, F., 2019. Preparedness against mobility disruption by floods. Science of the Total Environment, 654, pp.1010-1022.
6. Bhatt, C.M., Rao, G.S., Diwakar, P.G. and Dadhwal, V.K., 2017. Development of flood inundation extent libraries over a range of potential flood levels: a practical framework for quick flood response. Geomatics, Natural Hazards and Risk, 8(2), pp.384-401.
7. Singh, Y.K., Dutta, U., Prabhu, T.S., Prabu, I., Mhatre, J., Khare, M., Srivastava, S. and Dutta, S., 2017. Flood response system—a case study. Hydrology, 4(2), p.30.
8. Yildirim, E. and Demir, I., 2019. An integrated web framework for HAZUS-MH flood loss estimation analysis. Natural Hazards, 99(1), pp.275-286.
9. Lamichhane, N. and Sharma, S., 2017. Development of flood warning system and flood inundation mapping using field survey and LiDAR data for the Grand River near the city of Painesville, Ohio. Hydrology, 4(2), p.24.
10. Sermet, Y. and Demir, I., 2019b. Towards an information centric flood ontology for information management and communication. Earth Science Informatics, 12(4), pp.541-551.
11. Sermet, Y. and Demir, I., 2019a. Flood action VR: a virtual reality framework for disaster awareness and emergency response training. In ACM SIGGRAPH 2019 Posters (pp. 1-2).
12. Xiang, Z. and Demir, I., 2020. Distributed long-term hourly streamflow predictions using deep learning–A case study for State of Iowa. Environmental Modelling & Software, 131, p.104761.
13. Dettinger M. 2011. Climate change, atmospheric rivers, and floods in California – a multimodel analysis of storm frequency and magnitude changes. JAWRA Journal of the American Water Resources Association 47: 514–523.
14. Gaál L, Szolgay J, Kohnová S, Parajka J, Merz R, Viglione A, Blöschl G. 2012. Flood timescales: understanding the interplay of climate and catchment processes through comparative hydrology. Water Resources Research 48: W04511. DOI: 10.1029/2011WR011509.
15. Di Baldassarre G, Uhlenbrook S. 2012. Is the current flood of data enough? A treatise on research needs for the improvement of flood modelling. Hydrological Processes 26: 153–158.
16. Sermet, Y., Villanueva, P., Sit, M.A. and Demir, I., 2020b. Crowdsourced approaches for stage measurements at ungauged locations using smartphones. Hydrological Sciences Journal, 65(5), pp.813-822.

17. Seo, B.C., Keem, M., Hammond, R., Demir, I. and Krajewski, W.F., 2019. A pilot infrastructure for searching rainfall metadata and generating rainfall product using the big data of NEXRAD. Environmental modelling & software, 117, pp.69-75.

18. Ebert-Uphoff, I., Thompson, D.R., Demir, I., Gel, Y.R., Karpatne, A., Guereque, M., Kumar, V., Cabral-Cano, E. and Smyth, P., 2017, September. A vision for the development of benchmarks to bridge geoscience and data science. In 17th International Workshop on Climate Informatics.

19. Teng, J., Jakeman, A.J., Vaze, J., Croke, B.F., Dutta, D. and Kim, S., 2017. Flood inundation modelling: A review of methods, recent advances and uncertainty analysis. Environmental Modelling & Software, 90, pp.201-216.

20. Sit, M., Demiray, B.Z., Xiang, Z., Ewing, G.J., Sermet, Y. and Demir, I., 2020a. A comprehensive review of deep learning applications in hydrology and water resources. Water Science and Technology, 82(12), pp.2635-2670.

21. Esfandiari, M., Abdi, G., Jabari, S., McGrath, H. and Coleman, D., 2020. Flood Hazard Risk Mapping Using a Pseudo Supervised Random Forest. Remote Sensing, 12(19), p.3206.

22. Priestnall G, Jaafar J, Duncan A. 2000. Extracting urban features from LiDAR digital surface models. Computers, Environments and Urban Systems 24: 65–78.

23. Sinha S, Sotiropoulos F, Odgaard A. 1998. Three-dimensional numerical model for flow through natural rivers. Journal of Hydraulic Engineering 124: 13–24.

24. McGrath, H., Bourgon, J.F., Proulx-Bourque, J.S., Nastev, M. and El Ezz, A.A., 2018. A comparison of simplified conceptual models for rapid web-based flood inundation mapping. Natural Hazards, 93(2), pp.905-920.

25. Barthélémy, S., Ricci, S., Rochoux, M.C., Le Pape, E. and Thual, O., 2017. Ensemble-based data assimilation for operational flood forecasting–On the merits of state estimation for 1D hydrodynamic forecasting through the example of the "Adour Maritime" river. Journal of Hydrology, 552, pp.210-224.

26. Schumann, G., Bates, P.D., Apel, H. and Aronica, G.T., 2018. Global flood hazard mapping, modeling, and forecasting: challenges and perspectives. Global Flood Hazard: Applications in Modeling, Mapping, and Forecasting, pp.239-244.

27. Wu W, Rodi W, Wenka T. 2000. 3D numerical modeling of flow and sediment transport in open channels. Journal of Hydraulic Engineering ASCE 126(1): 4–15.

28. Afshari, S., Tavakoly, A.A., Rajib, M.A., Zheng, X., Follum, M.L., Omranian, E. and Fekete, B.M., 2018. Comparison of new generation low-complexity flood inundation mapping tools with a hydrodynamic model. Journal of Hydrology, 556, pp.539-556.

29. Gallant JC, Dowling TI. 2003. A multiresolution index of valley bottom flatness for mapping depositional areas. Water Resources Res. 39(12): 1347. DOI: 10.1029/2002WR001426.

30. Renno, C. D., Nobre, A. D., Cuartas, L. A., Soares, J. V., Hodnett, M., Tomasella, J., & Saleska, S. 2008. HAND, a new terrain descriptor using SRTM-DEM: Mapping terra-firme rainforest environments in Amazonia. Remote Sensing of Environment, 112 (9), 3469-3481.

31. Nobre, A. D., Cuartas, L. A., Hodnett, M., Renno, C. D., Rodrigues, G., Silveira, A., Waterloo, M., & Saleska, S. 2011. Height above the nearest drainage – a hydrologically relevant new terrain model. Journal of Hydrology, 404 (1-2), 13-29.

32. Nobre, A. D., Cuartas, L. A., Momo, M. R., Severo, D. L., Pinheiro, A., & Nobre, C. A. 2015. HAND contour: A new proxy predictor of inundation extent. Hydrological Processes.

33. Xu, H., Demir, I., Koylu, C. and Muste, M., 2019. A web-based geovisual analytics platform for identifying potential contributors to culvert sedimentation. Science of the Total Environment, 692, pp.806-817.

34. Sit, M., Langel, R.J., Thompson, D., Cwiertny, D.M. and Demir, I., 2020b. Web-based data analytics framework for well forecasting and groundwater quality. Science of The Total Environment, 761, p.144121.

35. Agliamzanov, R., Sit, M. and Demir, I., 2020. Hydrology@ Home: a distributed volunteer computing framework for hydrological research and applications. Journal of Hydroinformatics, 22(2), pp.235-248.

36. Sit, M., Sermet, Y. and Demir, I., 2019. Optimized watershed delineation library for server-side and client-side web applications. Open Geospatial Data, Software and Standards, 4(1), pp.1-10.

37. Haas, A., Rossberg, A., Schuff, DL., Titzer, BL., Holman, M., Gohman, D., Wagner, L., Zakai, A., Bastien, JF. 2017. Bringing the web up to speed with WebAssembly. Proceedings of the 38th ACM SIGPLAN Conference on Programming Language Design and Implementation, Barcelona, Spain, 2017. New York, NY: ACM.

38. Sermet, Y., Demir, I. and Muste, M., 2020a. A serious gaming framework for decision support on hydrological hazards. Science of The Total Environment, 728, p.138895.

39. Xu, H., Windsor, M., Muste, M. and Demir, I., 2020. A web-based decision support system for collaborative mitigation of multiple water-related hazards using serious gaming. Journal of environmental management, 255, p.109887.

40. Barnes, R., Lehman, C., & Mulla, D. 2013a. Priority-flood: An optimal depression-filling and watershed-labeling algorithm for digital elevation models. Computers & Geosciences, 62, 117-127.

41. Barnes, R., Lehman, C., & Mulla, D. 2013b. An efficient assignment of drainage direction over flat surfaces in raster digital elevation models. Computers & Geosciences, 62, 128-135.

42. Gilles, D., Young, N., Schroeder, H., Piotrowski, J. and Chang, Y.J., 2012. Inundation mapping initiatives of the Iowa Flood Center: Statewide coverage and detailed urban flooding analysis. Water, 4(1), pp.85-106.